PREDICTING EXPLOSION-GENERATED *Sn* AND *Lg* CODA USING SYNTHETIC SEISMOGRAMS

Ileana M. Tibuleac[1], Anastasia Stroujkova[1], Jessie L. Bonner[1], and Kevin Mayeda[2]

Weston Geophysical Corporation[1] and Lawrence Livermore National Laboratory[2]

Sponsored by National Nuclear Security Administration
Office of Nonproliferation Research and Engineering
Office of Defense Nuclear Nonproliferation

Contract No. DE-AC52-05NA26610[1] and W-7405-ENG-48[2]

ABSTRACT

Recent examinations of the characteristics of coda-derived *Sn* and *Lg* spectra for yield estimation have shown that the spectral peak of the Nevada Test Site (NTS) explosion spectra is depth-of-burial dependent, and that this peak is shifted to higher frequencies for Lop Nor explosions at the same depths. To confidently use coda-based yield formulas, we need to understand and predict coda spectral shape variations with depth, source media, velocity structure, topography, and geological heterogeneity. Thus, we have undertaken a coda modeling study to predict *Sn* and *Lg* coda.

During the initial stages of this research, we have acquired and parameterized deterministic 6º x 6º velocity and attenuation models for the Nevada, Shagan, Degelen, Novaya Zemlya, and Lop Nor Test Sites. Near-source data are used to constrain density and attenuation profiles for the upper five km at several test sites. The upper crust velocity profiles are quilted into a background velocity profile at depths greater than five km. Topography from digital elevation models will eventually be incorporated into the model development. The models are parameterized for use in a modified version of the Generalized Fourier Method in two and three dimensions (GFM2D/3D). The new GFM algorithm will soon include a coordinate transform that allows for variable gridding in the upper few kilometers of the model and simulation of the topography at finer scales. The smaller grid size in the upper crust allows for an increase in the accuracy of the *Sn* and *Lg* synthetics.

We are modifying these models to include stochastic heterogeneities of varying correlation lengths within the crust and upper mantle. Two parameters—correlation length and fractional velocity perturbation of the heterogeneities—are used to construct different realizations of random media. Multiple runs with different realizations of stochastic velocity are needed to calculate average amplitude envelopes of the seismic traces for every set of the stochastic parameters. We will calibrate these parameters by matching synthetic earthquake *Sn* and *Lg* coda envelopes to local earthquakes with well-defined moments and mechanisms.

Once the deterministic and stochastic models have been generated, we will use GFM2D/3D to generate regional-distance synthetics for monopole explosions at depths ranging from 0.25 to 1 km for all test site models. We will then superimpose secondary source effects, such as spall and compensated linear-vector dipole (CLVD) sources, on the monopole synthetics. Finally, we will derive *Sn* and *Lg* coda spectra from the synthetics, estimate moments and yields from these spectra, and compare to observed data from each test site. If successful, this method may be used to estimate the *Sn* and *Lg* coda properties for yield estimation of explosions at historical test sites or for broad, uncalibrated regions where we will likely have little information on velocity structure.

OBJECTIVE

Our objective is to determine why the current mechanisms for *Sn* and *Lg* generation from explosions often produce stable coda magnitudes that are transportable between test sites. We aim to understand and predict *Lg* and *Sn* coda spectral shapes with variations in source depth, material properties, velocity structure, topography, and geological heterogeneity. We will use 2-D and 3-D modeling techniques to estimate synthetic explosion coda for five nuclear test sites as well as for regions without nuclear testing history.

RESEARCH ACCOMPLISHED

For sparse local and regional seismic networks and small events (< ~1 kt), one of the most stable and unbiased methods for yield and magnitude estimation is based on *Sn* and *Lg* coda envelopes (Mayeda, 1993). Coda-derived spectra have characteristics that require in-depth investigation so that any possible bias can be accounted for when lower bounds on yields are reported by U. S. monitoring agencies. For example, the peaks of coda-derived Nevada Test Site (NTS) and Lop Nor explosion spectra are depth-of-burial dependent; however, the peaks are shifted to higher frequencies at Lop Nor.

We are in the first phase of a research program in which we plan to compare observed local and regional *Sn* and *Lg* coda spectra to coda-derived source spectra for simulated explosions at the Nevada (NTS), Shagan (STS), Degelen (DTS), Novaya Zemlya (NZ), and Lop Nor (LN) test sites. We aim to develop a physical understanding of these data. We are currently developing a methodology consisting of 1) compilation and parameterization of deterministic material models for each test site; 2) addition of stochastic perturbations of variable correlation lengths to the deterministic model parameters; 3) calibration of stochastic variations at each test site using nearby earthquake data, and 4) calculation of 2-D/3-D synthetics for composite source models of varying depths and moments for each test site. Synthetic waveforms are created using a Generalized Fourier Method (GFM; Orrey et al., 2002). An illustration of our progress in developing this methodology is presented below with preliminary results for a simulated explosion at the Shagan Test Site.

1) Development of Velocity Models

Deterministic models. We are compiling deterministic velocity and attenuation models for the upper crust at five test sites (Table 1). Near-source data is used to constrain the *P, S,* density, and attenuation profiles for the upper 5 km at each test site. These upper crustal velocity profiles are "quilted" into a background velocity profile for each test site at depths greater than five km. We combine several background velocity models including the global 1°x1° models of Stevens and Adams (1999), the CRUST2.0 models of Bassin et al. (2000) and regionalized models (such as the regionalized background model for eastern Kazakhstan, Priestley et al., 1998). Each velocity model is parameterized for use in GFM2D/3D with a grid spacing of either 0.25 or 0.5 km.

Table 1. References for deterministic velocity and attenuation models for the upper crust at several test sites. Center coordinates of each test site are also listed.

Test Site	Abbreviation	References
Nevada Test Site (Pahute and Yucca) 37.148 N, 116.215 W	NTS	McLaughlin et al. (1983); Stump and Johnson (1984); Ferguson et al. (1994); Stevens et al., (1991); Mankinen et al. (2003); Benz et al., (1991)
Semipalatinsk (Shagan) 49.940 N, 78.862 E	STS	Bonner et al. (2001); Kazakh NNC Report (1996); Davis and Berlin (1992); Priestley et al. (1988)
Semipalatinsk (Degelen) 49.940 N, 78.048 E	DTS	Priestley et al. (1988); Belyashova et al. (2001)
Lop Nor 41.669 N, 88.703 E	LN	Kosarev et al., (1993); Burchin et al. (2001); Fisk, (2002); Waldhauser and Richards (2004).
Novaya Zemlya 73.335 N, 54.716 E	NZ	Kremenetskaya et al. (2001); Bowers (2002); Bungum et al. (2004)

Examples of 1D profiles of *P* and *S* velocity models of the five test sites are shown in Figure 1. The background velocity structure and the velocities in the upper crust are based on information provided by the references in Table 1. For example, the background velocity structure for the STS (left upper plot, dotted line) is based on a regional model for eastern Kazakhstan developed by Priestley et al. (1988). The velocities in the upper crust are based on borehole data (National Nuclear Center Nuclear Report) and *Rg* inversions (Bonner et al., 2001). The right upper plot shows a velocity profile at Pahute Mesa, at NTS. Examples of 1D profiles of *P* and *S* velocity models at the NZ and LN test sites are shown the lower plots of Figure 1. All models extend to 50 km in the horizontal direction and to at least 200 km in the vertical direction.

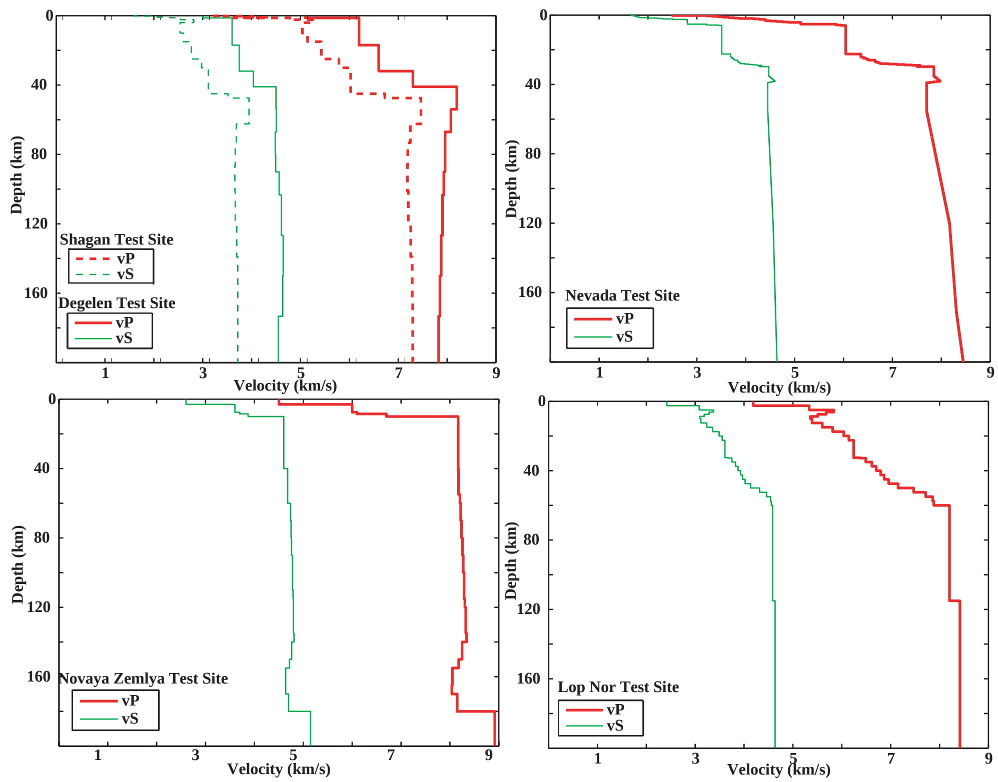

Figure 1. Examples of preliminary deterministic models for the Semipalatinsk (Shagan and Degelen) Test Sites (upper left plot), Nevada (upper right plot), Novaya Zemlya (lower left plot), and Lop Nor (lower right plot) test sites.

Stochastic models. The deterministic models are perturbed by adding random heterogeneities with predefined stochastic properties, obtained using the method of Frankel and Clayton (1986). A random number generator is used to create velocity perturbations at each point in the 2D or 3D deterministic velocity model. The random velocity perturbation field is then Fourier transformed to wave number space, filtered to achieve the desired spectrum (e.g., correlation distances), and transformed back to the velocity field. The perturbations are subsequently scaled to the desired amplitude and added to the 2D or 3D deterministic velocity field.

Three types of filters are commonly used to describe real geologic media: exponential, Gaussian, and von Karman (Table 2 and Figure 2). Velocity variations are well described by the von Karman self-similar autocovariance function (Frankel and Clayton, 1986; Levander and Hollinger, 1992; Pullammanappallil et al., 1997); therefore, we have chosen this function to describe our initial stochastic models.

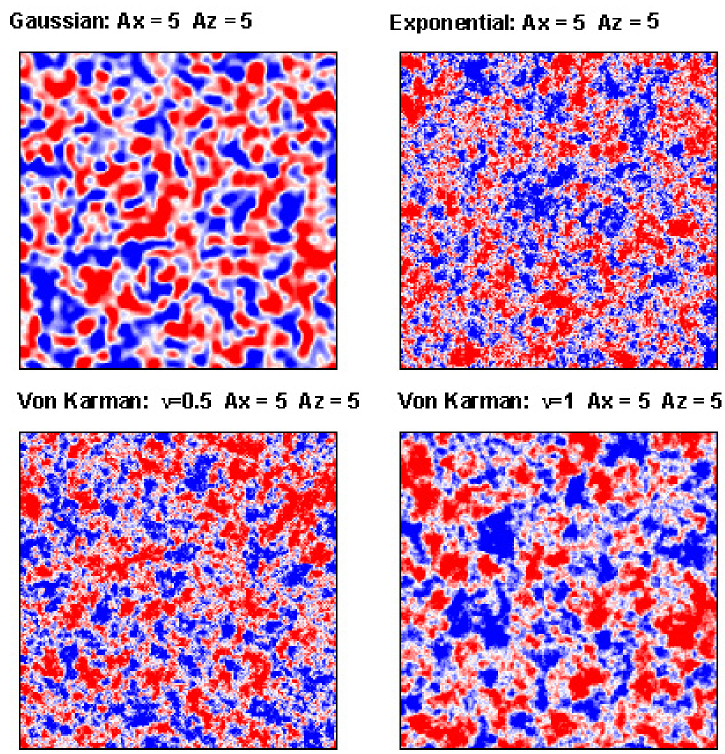

Figure 2. Random perturbation field examples obtained by using the filters listed in Table 2 on a 256 x 256 pixel block. The perturbations are scaled to the desired amplitude and added to the deterministic velocity field.

Table 2. Filters applied to the random perturbation field, where *a* is a characteristic correlation length of the medium and *v* is the Hurst number, related to the fractal dimension of the medium.

Filter	Spatial covariance function C
Gaussian	$C_g = \exp(-r^2/2a^2)$
Exponential	$C_e = \exp(-r/a)$
von Karman	$C_k = r^{\nu} K_{\nu}(r)$

To address the nonuniqueness inherent in our method, correlation functions for scattering at each test site are restricted to be within the bounds of the results from literature searches and satellite imagery correlation-length analyses. Nearby earthquakes with well-defined focal mechanisms can also be used, where available, to provide us with bounds on the scattering in our model.

Figure 3 is an example of this methodology applied to the Shagan velocity model shown in Figure 1, left upper plot. The correlation length for this model was chosen to be 1.5 km with 10% velocity variations.

2) Methodology illustration for an explosion at the Shagan Test Site

We superpose a 0.5 km deep explosion with a smaller Compensated Linear Vector Dipole (CLVD) source at a depth of 0.2 km, and present the results at a distance of 310 km. Figure 4 provides a comparison of the composite source synthetics (CLVD+Explosion Monopole) calculated using a model with and without random velocity variations (Figure 3). In the upper plot, we note that there are large high-frequency surface waves (> 2 Hz) that are typically not observed in regional data from explosions at the Shagan Test Site. The Q value used in the upper crust was less than 100; however, it did not decrease the amplitudes of these surface waves. But, adding the crustal heterogeneity (lower plot) *does* remove these surface waves by forward- and back- scattering the energy into the *Lg* coda. The synthetic seismogram in the lower plot of Figure 4 shows that coda resembling regional recordings can be generated using our methodology.

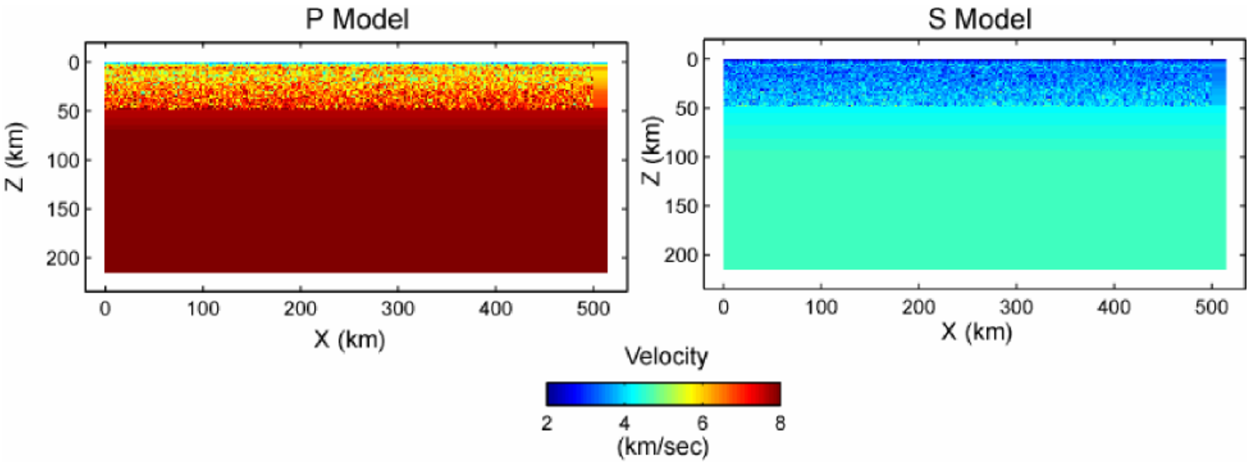

Figure 3. Example of combined deterministic and stochastic *P*- and *S*-wave models for the Shagan Test Site in Kazkahstan. The background velocity structure is shown in Figure 1, left upper plot, dotted line. Stochastic variations with correlation lengths of 1.5 km and 10% velocity perturbations were added using the methods of Frankel and Clayton (1986).

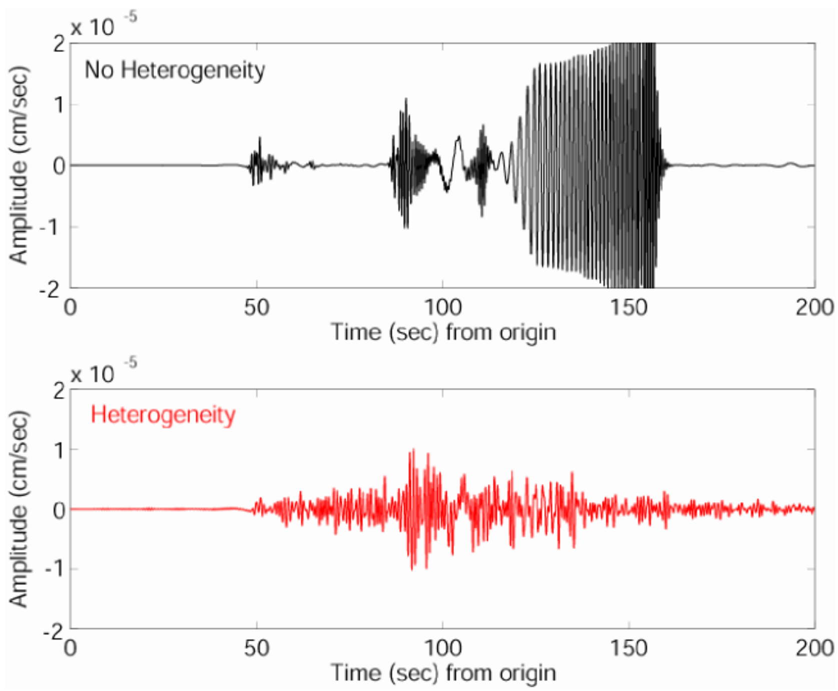

Figure 4. A comparison of synthetics for a composite explosion plus CLVD source in a Shagan test site velocity model without (upper) and with (lower) stochastic variations. In the lower plot, the *Lg* coda behaves very similarly to regional recordings of explosions at the Shagan Test Site.

Coda processing is performed using the coda software described in detail in Mayeda et al. (2003). An example of this processing as applied to the synthetic waveforms shown in Figure 4 is provided in Figure 5. While we show only the first 200 seconds of the synthetics in Figure 4, the analysis in Figure 5 is for 800 seconds of data. For the velocity model with no stochastic heterogeneities, we do not see appropriate coda behavior in the processing. The peaks associated with the *Lg* and *Rg* arrivals are observed, and then the amplitudes rapidly approach pre-event noise levels by 200 seconds after event origin. For the synthetics with stochastic heterogeneities, we observe appropriate coda behavior, as the amplitudes do not approach the background noise levels until 500 seconds after the event origin. The coda behavior in different frequency bands is very similar to the lower-frequency type coda amplitude curves proposed for the Shagan test site by Phillips et al. (2004).

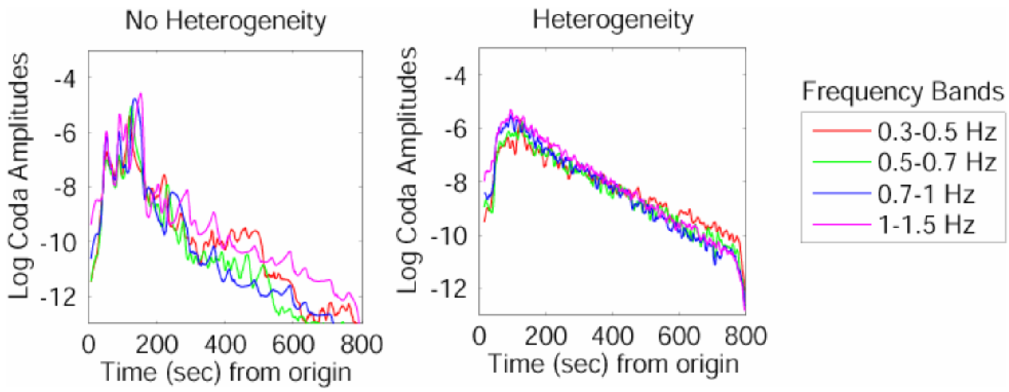

Figure 5. Examples of coda processing on synthetic seismograms without (left) and with (right) random velocity heterogeneities in the model. The coda amplitudes on the right are very similar to the type coda amplitude curves proposed for the Shagan Test Site by Phillips et al. (2004).

The next stage of modeling development will be the addition of topography. GFM2-D/3-D is undergoing modifications to include topography. We will use digital elevation models for all test sites in order to simulate *Rg* scattering from topography, which has been shown to be a primary constituent of explosion-generated shear waves. This scattering will contribute to the coda signatures for our synthetics. We will then systematically modify the random velocity heterogeneities to improve the match between the observed and synthetic data. 3D strip models will also be developed to examine scattering efficiency of 2-D media in comparison to 3-D simulations.

CONCLUSIONS AND RECOMMENDATIONS

In this paper we present preliminary results from a study which aims to develop a methodology for modeling *Sn* and *Lg* coda-derived source spectra for simulated explosions at the Nevada, Shagan, Degelen, Novaya Zemlya and Lop Nor test sites. Using synthetic seismograms at the Shagan Test Site we show that coda resembling regional recordings of explosions at the Shagan Test Site can be generated using a combination of deterministic and stochastic models.

In the future we will use GFM to propagate synthetics from compound explosion and CLVD sources to epicentral distances of up to 600 km in both 2D and 3D models. These waveforms will be used to generate coda-derived *Lg* and *Sn* spectra in order to estimate the magnitudes and yields for the synthetic events. We will compare the spectral peaks from different depths of burial and examine any similarities to observations. We will quantify possible biases in the yields between test sites and relate them to the choice of, or combination of, *Sn* and *Lg* mechanisms. Finally, we will use our techniques to estimate the *Sn* and *Lg* coda spectra for explosions in uncalibrated regions. We will use available earthquake data, digital elevation models, and satellite imagery to determine the properties of the stochastic models, so that explosion-generated coda spectra for uncalibrated regions can be estimated.

ACKNOWLEDGMENTS

We wish to thank Dr. Jeffrey Orrey for his continued support on the GFM2D/3D code. We express our gratitude to Heather Hooper for help editing this paper and to James Britton for help with ArcView figure plots.

REFERENCES

Bassin, C., G. Laske, and G. Masters (2000), Current limits of resolution for surface wave tomography in North America. *EOS Trans AGU.* 81: F897.

Belyashova, N. N., V. I. Shacilov, N. N. Mikhailova, I. I. Komarov, Z. I. Sinyova, A. V. Belyashov, and M. N. Malakhova (2001), On the use of calibration explosions at the former Semipalatinsk test site for compiling a travel-time model of the crust and upper mantle. *Pure Appl. Geophys.* 158: 193-209

Benz, H. M., Unger, J. D., Leith, W., and V. Ryaboy (1991), The Norilsk DSS Profile in Northern Siberia: Interpretation of the velocity structure and comparison with Basin and Range and New England profiling results, Abstracts of the 13'th Annual PL/DARPA Seismic Research Symposium, 85–100.

Bonner, J., D.C. Pearson, W.S. Phillips, and S.R. Taylor (2001), Shallow velocity structure of the Shagan River Test Site in eastern Kazakhstan. *Pure Appl. Geophys.* 158: 2017–2039.

Bowers, D. (2002), Was the 16 August 1997 Seismic Disturbance near Novaya Zemlya an Earthquake? *Bull. Seis. Soc. Am.* 92: 2400–2409.

Bungum, H., O. Ritzmann, J. Faleide, N. Maercklin, J. Schweitzer, W. Mooney, S. Detweiler, and W. Leith (2004), Development of a Three-dimensional Velocity Model for the Crust and Upper Mantle in the Barents Sea, Novaya Zemlya, Kara Sea and Kola-Karelia Regions, in *Proceedings of the 26th Annual Seismic Research Review on Nuclear Monitoring Technologies,* LA-UR-04-5801, Orlando, FL.

Burchin, B. G., A. Z. Mostinsky, A. A. Egorkin, A. L. Levhin, and M. H. Ritzwoller (2001), Isotropic and nonisotropic components of earthquakes and nuclear explosions on the Lop Nor Test Site, China, *Pure Appl. Geophys.* 158: 1497–1515.

Davis, P. A. and G. L. Berlin (1992), Geologic mapping of the Semipalintisk region using Land Sat thematic mapper and spot panochromatic data, LA-UR-92-310: 15.

Ferguson, J. F., A. H. Cogbill, and R. G. (1994), A geophysical-geological transect of the Silent Canyon caldera complex, Pahute Mesa, Nevada, *J. Geophys. Res.* 99: 4323–4339.

Fisk, M. D. (2002), Accurate locations of nuclear explosions at the Lop Nor Test Site using alignment of seismograms and IKONOS satellite imagery. *Bull. Seis. Soc. Am.* 92: 2911–2925.

Frankel, A. and R. W. Clayton (1986), Finite difference simulations of seismic scattering: implications for the propagation of short-period seismic waves in the crust and models of crustal heterogeneity. *J. Geophys. Res.* 91. (B6): 6465–6489.

Levander, S. A., and K. Hollinger (1992), Small-scale heterogeneity and large-scale velocity structure of the continental crust, *J. Geophys. Res.* 97: 8797–8804.

Kazakh NNC Report (1996), Unused vertical boreholes at the Balapan test field of the former Semipalantinsk test site: review of existing data on the boreholes geology and design, *National Nuclear Center of the Republic of Kazakhstan Report*.

Kosarev, G. L., Petersen, N. V. and L. P. Vinnik (1993), Receiver functions for the Tien Shan analog broadband network: contrasts in the evolution of structures across the Talasso-Fergana fault, *J. Geophys. Res.* 98: 4437–4448.

Kremenetskaya, E., V. Asming and F. Ringdal (2001), Seismic location calibration of the European Arctic, *Pure Appl. Geophys.* 158: 117–128.

Mankinen, E. A., T. G. Hildenbrand, C. J. Fridrich, E. H. McKee and C. J. Schenkel (2003), Geophysical setting of the Pahute Mesa-Oasis Valley region, Southern Nevada, Report 50, Nevada Bureau of Mines and Geology, University of Nevada: 12–13.

Mayeda, K. M. (1993),mb(*Lg*Coda): a stable single station estimator of magnitude, *BSSA,* 83: 851–861.

Mayeda, K., A. Hofstetter, J.L. O'Boyle, and W.R. Walter (2003), Stable and transportable regional magnitudes based on coda-derived moment-rate spectra, *Bull. Seis. Soc. Am.* 93: 224–239.

McLaughlin, KL, L. R. Johnson, LR and T.V. McEvilly (1983), Two-dimensional array measurements of near-source ground accelerations. *Bull. Seis. Soc. Am.* 73: 349–375.

Orrey, J. L., C. B. Archambeau and G. A. Frazier (2002), Complete seismic wavefield synthesis with a pseudospectral method: The Generalized Fourier Method, revised manuscript to be submitted to *Geophys. J. Int.*

Phillips, W., H. Patton, S. Taylor, H. Hartse, and G. Randall (2004), Calibration for coda based magnitude and yield, in *Proceedings of the 26th Annual Seismic Research Review on Nuclear Monitoring Technologies,* LA-UR-04_5801, Orlando, FL.

Priestley, K. F., G. Zandt, and G. E. Randall (1988), Crustal structure in Eastern Kazakh, USSR from teleseismic receiver functions. *Geophys. Res. Lett.* 15: 613–616.

Pullammanappallil, S., A. Levander, S. Larkin (1997), Estimation of crustal stochastic parameters from seismic exploration data, *J. Geophys. Res.* 102: 15,269–15,286.

Stevens, J. L. and D. A. Adams (1999), Improved methods for regionalized surface wave analysis. *Proceedings of the 21st Annual Seismic Research Symposium,* Las Vegas, NV.

Stevens, J. L., T. G. Berker, S. M. Day, K. L. McLaughlin, N. Rimer, and B. Shkoller (1991), Simulation of teleseismic body waves, regional seismograms, and Rayleigh wave phase shifts using two-dimensional, nonlinear models of explosion sources, *Explosion Source Phenomenology, Geophysical Monograph 65*, Copyright 1991, American Geophysical Union: 239–252.

Stump, B.W. and L. Johnson (1984), Near-field source characterization of contained nuclear explosions in tuff, *Bull. Seis. Soc. Am.* 74: 1–26.

Waldhauser, F. and P. G. Richards (2004), Reference events for regional seismic phases at IMS stations in China, *Bull. Seis. Soc. Am.* 94: 2265–2279.